Vibrioferrin production by the food spoilage bacterium *Pseudomonas fragi*

Tamsyn Stanborough[a, b], Narelle Fegan[a], Shane M. Powell[b], Mark Tamplin[b] and P. Scott Chandry[a,#].

[a] CSIRO Agriculture and Food, Werribee, Victoria, Australia

[b] Centre for Food Safety and Innovation, Tasmanian Institute of Agriculture, University of Tasmania, Hobart, Tasmania, Australia

[#] Address correspondence to Scott Chandry: CSIRO Agriculture and Food, 671 Sneydes Road, Werribee, 3030, Victoria, Australia, Tel: +61 3 9731 3312, Fax: +61 3 9731 3201, Email: Scott.Chandry@csiro.au

One sentence summary: *Pseudomonas fragi* produces a vibrioferrin siderophore that plays a role in iron acquisition under low iron conditions.

ABSTRACT

Pseudomonas fragi is a meat and milk spoilage bacterium with high iron requirements, however mechanisms of iron acquisition remain largely unknown. The aim of this work was to investigate siderophore production as an iron acquisition system for *P. fragi*. A vibrioferrin siderophore gene cluster was identified in 13 *P. fragi* and experiments were conducted with a representative strain of this group (F1801). Chromeazurol S assays showed *P. fragi* F1801 produced siderophores under iron starvation at optimum growth and refrigeration temperature. Conversely, supplementation of low iron media with 50 µM $FeCl_3$ repressed transcription of the vibrioferrin genes and siderophore production. Disruption of the siderophore receptor

(*pvuA*) caused polar effects on downstream vibrioferrin genes, resulting in impaired siderophore production of the Δ*pvuA* mutant. Growth of this mutant was compared to growth of a control strain (Δ*lip*) with wild-type vibrioferrin genes in low iron media supplemented with iron chelators 2,2'-bipyridyl or apo-transferrin. While 25 µM 2,2'-bipyridyl caused impaired growth of Δ*pvuA*, growth of the mutant was completely inhibited by 2.5 µM apo-transferrin, but could be restored by $FeCl_3$-addition. In summary, this work identifies a vibrioferrin-mediated iron acquisition system of *P. fragi*, which is required for growth of this bacterium under iron-starvation.

Keywords

Pseudomonas fragi; siderophore; vibrioferrin; food spoilage; iron acquisition; iron chelators

INTRODUCTION

Iron is required for fundamental cellular processes such as respiration and the synthesis of amino acids and DNA, and is therefore an essential element for the majority of microorganisms (Ilbert and Bonnefoy 2013). However, iron is in short supply in many habitats. For example, in aerobic environments at neutral pH, Fe^{2+} is rapidly oxidized to Fe^{3+}, leading to the formation of insoluble hydroxide salts and rendering iron scarce in the environment (Colombo*, et al.* 2014). Similarly, in the human host and foods such as milk and meat, iron is sequestered by iron-binding proteins including transferrin family proteins, transferrin and lactoferrin, hemeproteins myoglobin and haemoglobin, and ferritin (Skaar 2010).

Microorganisms have evolved a variety of mechanisms to obtain their iron. In iron-rich environments, iron acquisition occurs through energy-independent, low-affinity iron uptake systems (Jones and Niederweis 2010). In iron-limited environments, a common strategy involves the excretion of small molecular weight iron chelating compounds termed siderophores (Noinaj*, et al.* 2010). Fe^{3+}-siderophore complexes that form outside the cell are taken up in Gram-negative bacteria by specific outer membrane receptors, which are supplied with energy for transport from the cytoplasmic membrane by the Ton system (Faraldo-Gomez and Sansom 2003).

Excess iron causes toxic cellular effects, necessitating the tight regulation of iron uptake in microorganisms. The Ferric Uptake Regular protein (Fur) regulates iron homoeostasis at the transcription level in many Gram-negative and some Gram-positive organisms (Carpenter*, et al.* 2009). When intracellular Fe^{2+}-concentrations exceed a certain threshold level, Fur binds to specific regulatory DNA sequences, termed Fur-boxes, preventing RNA polymerase binding to promotors (Troxell and Hassan 2013). In contrast, scarcity of intracellular iron causes Fur to lose its ability to bind to Fur-boxes, resulting in gene transcription. Thus, the transcription of iron uptake genes is ultimately regulated by the concentration of intracellular iron.

Pseudomonas have some of the best studied siderophore-mediated iron uptake systems such as the pyoverdine siderophores of the fluorescent pseudomonads (Cezard*, et al.* 2015, Cox and Adams 1985, Meyer and Abdallah 1978, Trapet*, et al.* 2016). In contrast, *Pseudomonas fragi* has been considered a non-siderophore producing member of this genus and is described as not producing siderophores in detectable amounts in Bergey's Manual (Champomier-Vergès*, et al.* 1996, Garrity*, et al.* 2005). *P. fragi* is a problematic meat and milk spoilage bacterium with high iron requirements, but beyond its ability to scavenge foreign Fe^{3+}-siderophore

complexes, very little is known about the strategies this bacterium employs to obtain iron (Casaburi*, et al.* 2015, Champomier-Vergès*, et al.* 1996, De Jonghe*, et al.* 2011). Interestingly, in a recent study on plant-growth promoting bacteria, a putative *P. fragi* isolate derived from the rhizosphere was shown to produce siderophores (Farh*, et al.* 2017), suggesting previous conclusions that this bacterium is a non-siderophore producer may not have been accurate.

In this work, siderophore production was investigated as an iron acquisition system for *P. fragi*. The genomes of 13 *P. fragi* were examined for the presence of siderophore biosynthetic gene clusters, which led to the identification of vibrioferrin biosynthesis and vibrioferrin-mediated iron acquisition genes. This work describes experiments that determine siderophore production for *P. fragi* F1801 and show a role for the siderophore in iron metabolism of this bacterium under low iron conditions.

MATERIALS AND METHODS

Strains, plasmids and growth conditions

Strains, plasmids, and genome and gene sequences used in this study are included in Table 1.

Conditions of iron starvation were achieved in modified M9 media (MM9) comprising 10% v/v of MM9 salts (5 g/L NaCl, 10 g/L NH_4Cl, 0.59 g/L $Na_2HPO_4.H_2O$ and 0.45 g/L KH_2PO_4), 2 mM $MgSO_4$, 0.1 mM $CaCl_2$, 0.2% w/v glucose, 0.3% casamino acids w/v, 0.2% w/v succinate and 0.1 M PIPES (pH 6.8, NaOH). *P. fragi* cultures were grown under agitation unless otherwise specified. Kanamycin was added to culture media of gene disruption mutants at a concentration of 50 µg/ml.

Identification of siderophore gene cluster

Examination of the 13 previously sequenced *P. fragi* genomes (Table 1) for siderophore biosynthetic gene clusters was performed with antiSMASH version 4 (Blin*, et al.* 2017).

Generation of disruption mutants, genomic DNA isolation, and genome sequencing and analysis

A gene disruption mutant was generated of the TonB-dependent outer membrane siderophore receptor (Δ*pvuA*) by homologous recombination with a pJP5603 suicide vector construct. This system results in a single cross-over event, whereby the pJP5603 vector (Riedel*, et al.* 2013) encoding a kanamycin resistance gene remains integrated in the genome (Penfold and Pemberton 1992). Thus, a control strain with wild-type vibrioferrin genes and a disrupted lipase gene (Δ*lip*) was generated for subsequent experimental comparisons. The *lip* gene was chosen because the disruption of this gene would not affect iron metabolism of the strain, nor would it be required for growth of the strain in the culture media used in this work. Further, because it is present as single gene rather than in an operon cluster, polar effects on downstream genes were highly unlikely.

DNA manipulations were performed using standard protocols (Sambrook and Russell 2001). Plasmid constructs were generated by ligating *BamHI*-digested pJP5603 and *BamHI*-restriction fragments of the *P. fragi* F1801 *lip* and *pvuA* genes (Table 1), which were amplified using primers included in Table S1.

pJP5603 gene disruption constructs were transferred from *E. coli* S17-1 *λpir* (Simon*, et al.* 1983) to *P. fragi* F1801 by biparental filter matings as previously described

(Windgassen*, et al.* 2000) with some adjustments; recipient cells were grown at 30°C and the ratio of donor to recipient cells was 1:2 ($5x10^8$ CFU to 10^9 CFU), respectively. After mating, cells were spread on *Pseudomonas* agar containing cetrimide-fucidin-cephaloridine selective supplement (Oxoid) for *Pseudomonas* and 50 µg/mL kanamycin sulphate to select for transconjugants. Plates were incubated at 25°C for 30 h.

Strains (wild-type F1801, Δ*lip* and Δ*pvuA*) were grown for 18 h in tryptone soya broth (TSB, Oxoid) at 25°C. Genomic DNA was isolated with the DNeasy Blood and Tissue Kit (QIAGEN) according the manufacturer's protocol for Gram-negative bacteria. Library preparation and genome sequencing was carried out at Queensland Health (Health Support Queensland) using MiniSeq High Output kits with 150 cycles and the Illumina MiniSeq System (Illumina). Genome assembly was performed as previously described (Stanborough*, et al.* 2017). Confirmation of correct insertion of the vector was achieved by manual inspection of the genomes with Geneious version 9.0.5 (Kearse*, et al.* 2012). Snippy (https://github.com/tseemann/snippy) was used to confirm an absence of additional genetic variants in the Δ*lip* and Δ*pvuA* mutants' genomes by aligning sequence reads of wild-type F1801, Δ*pvuA* and Δ*lip* strains to the reference genome of F1801.

Sequence reads of wild-type F1801, Δ*lip* and Δ*pvuA* strains were deposited in the Sequence Read Archive and the respective accession numbers are provided in Table 1.

Phylogenetic tree of vibrioferrin sequences

MAFFT multiple sequence alignments (Katoh*, et al.* 2002) of the vibrioferrin PvuA and PvsA-PvsE protein sequences were performed using the default settings. The

six multiple alignments were concatenated and Gblocks version 0.91b (Castresana 2000, Talavera and Castresana 2007) was run with the default settings to remove poorly aligned positions and divergent regions of the alignments. Bayesian inference (BI), performed with MrBayes version 3.2.6 (Ronquist and Huelsenbeck 2003), was conducted with a run of 1000,000 generations and sampling every 1000. A mixed amino acid model analysis was set, enabling the MCMC sampler to test all of the fixed rate models. MrBayes determined that the Wheeler and Goldman (WAG) model of amino acid replacement (Whelan and Goldman 2001) had the best likelihood score and was chosen for the analysis. Convergence parameters were assessed using Tracer version 1.6 (Rambaut*, et al.* 2014) and the majority rule consensus tree was rendered with Figtree version 1.4.2 (Morariu*, et al.* 2009). BIs were run three times to ensure reproducibility of the resulting trees.

RNA isolation and quantitative reverse transcription-polymerase chain reaction (qRT-PCR)

RNA was isolated from 1 ml of mid-log phase iron-starved cultures ($1.5x10^8$ CFU). Stabilisation of RNA was achieved with RNAprotect Bacteria Reagent (QIAGEN) following the manufacturer's recommendations and total RNA was extracted with the RNeasy Mini Kit (QIAGEN) according to the supplier's instructions and stored in H_2O at -80°C. cDNA was synthesised from 1 µg of total RNA using iScript gDNA Clear cDNA Synthesis Kit (Biorad) as suggested by the manufacturer, however DNase treatment was increased from the recommended 5 to 30 min. qRT-PCR was performed on an AriaMx Real-time PCR System (Agilent) using the iTaq Universal SYBR Green Supermix (Biorad) as a fluorescence source. PCR reaction mixes included 10 µl iTaq Universal SYBR Green Supermix (Biorad), 500 nM forward and reverse primers and 1 µl template cDNA (diluted 1:10 in H_2O) in a total volume of 20

µL. Primer sequences, provided in Table S1, were designed with Primer3 version 2.3.4 (Untergasser*, et al.* 2012) . Acceptable primer efficiency was confirmed for each target gene with standard curves, and melt-curve analysis of amplicons of each target gene was performed to ensure amplification of single gene products. PCR conditions were: 30 s at 95°C followed by 40 cycles of 5 s at 95°C and 30 sec at 60°C. Melt-curve analysis involved an incremental increase of 0.5°C every 2 s from 65 to 95°C. Each assay included a non-template control, and each sample a control without reverse transcriptase. Raw data were analysed with Agilent AriaMx version 1.0 software and exported to excel for further analysis. Ct-values were normalised to the isocitrate dehydrogenase gene (gene locus tag CJU81_09775 in F1801, GenBank accession no. GCA_002269505.1) and relative expression levels were calculated according to the $2^{\Delta\Delta Ct}$ method.

Chromeazurol S (CAS) supernatant assays

CAS assay solution was prepared as previously described (Alexander and Zuberer 1991). Siderophore detection from culture supernatants was performed using the method of Schwyn and Neilands (1987). Briefly, bacterial cultures were spun down at 2,500 x g for 5 min and the supernatants were filtered through a 0.20 µm cellulose acetate membrane filter (Sartorius). Siderophores were detected in the supernatants by mixing equal volumes of filtered supernatant and CAS solution. After allowing the solutions to equilibrate for 1.5 h, a visible change in the colour of the mixture from blue to orange was considered a positive reaction. To detect siderophore production at 25°C, strains were grown in 4 ml MM9 for 18 h prior to supernatant collection. To monitor siderophore production at 4°C, F1801 was grown in 50 ml MM9 for 4 d and every 24 h 3 ml of culture were removed to measure growth (A_{600}), and detect siderophores by CAS supernatant assays. To monitor the increase in siderophore

levels over the 4 d, absorbance measurements of the CAS reaction mixtures were performed at 630 nm.

Growth experiments with 2,2'-bipyridyl and bovine apo-transferrin

Single colonies were used to inoculate 3 ml MM9. Cultures were grown at 25°C for 18 h. 20 µl of these cultures were used to inoculate 180 µl fresh MM9, supplemented as indicated in the text with 2,2'-bipyridyl (Sigma-Aldrich), bovine apo-transferrin (Sigma-Aldrich) and/or sodium bicarbonate and $FeCl_3$, in Greiner 96-well flat bottom microtiter plates (Sigma-Aldrich). Growth was monitored (A_{600}) using an EON microplate reader (BioTek).

RESULTS AND DISCUSSION

In this work, 13 previously sequenced *P. fragi* genomes were examined for the presence of siderophore biosynthetic gene clusters. This search resulted in the identification of a conserved gene cluster, homologs of which were shown to be responsible for vibrioferrin biosynthesis and vibrioferrin-mediated iron uptake in the terrestrial bacteria *Azotobacter vinelandii* and *Xanthomonas* spp., and in the marine bacterium *Vibrio parahaemolyticus* (Baars*, et al.* 2016, Pandey and Sonti 2010, Pandey*, et al.* 2017, Yamamoto*, et al.* 1994) (Fig 1). Similar to the vibrioferrin gene clusters in *A. vinelandii* and *X. campestris*, this ~10 kb region in *P. fragi* comprised seven open reading frames (Fig 1A). Previous work in *Xanthomonas* spp. and *V. parahaemolyticus* showed five of these genes (*mhpE*, *pvsA*, *pvsB*, *pvsD* and *pvsE*) are involved in the biosynthesis of vibrioferrin, while *pvuA* is a TonB-dependent outer-membrane receptor and *pvsC* an inner-membrane exporter for vibrioferrin (Fujita*, et al.* 2011, Funahashi*, et al.* 2002, Pandey and Sonti 2010, Tanabe*, et al.* 2006). Locus tags of these genes in the 13 strains are shown in Table 1. Analysis of

the upstream region of this gene cluster revealed the presence of a 19 bp sequence, matching 14 of the 19 nucleotides of the *Xanthomonas campestris* consensus Fur-box (Blanvillain*, et al.* 2007) and 11 of the 19 nucleotides of the *Escherichia coli* and *Pseudomonas aeruginosa* consensus Fur-box. This sequence was located 129 bases upstream of the *mhpE* start codon. Fur homologs were also identified in the *P. fragi* genomes with the locus-tag CJU81_16820 in F1801.

To investigate the relatedness of the vibrioferrin genes between the 13 strains and *A. vinelandii*, *X. campestris* and *V. parahaemolyticus*, a phylogenetic tree of the PvuA and PvsA-PvsE sequences was determined by Bayesian inference (BI) (Fig 1B). Topology of the BI consensus tree showed three clades of *P. fragi* vibrioferrin sequences. The largest of the three clades, comprising closely related sequences of eight of the 13 strains, was clearly separated from the other two clades, which share a more recent common ancestral sequence. The sequences of the *P. fragi* type strain were found in one of these two clades with those of two additional strains. Sequences of F1801, the *P. fragi* strain used for subsequent experiments, were grouped together in the second of these clades with vibrioferrin sequences of one other strain. In accordance with their phylogeny, sequences of the *P. fragi* were closest to those of *A. vinelandii*, while those of *X. campestris* and *V. parahaemolyticus* were substantially more distant.

Previous work suggested that *P. fragi* does not synthesise siderophores (Champomier-Vergès*, et al.* 1996), and utilising the succinate media (non-deferrated and deferrated forms) presented in the work, *P. fragi* F1801 displayed little to no growth and siderophore production of this strain was not observed (data not shown). Therefore in this study, a non-deferrated, modified M9 medium (MM9) was used containing glucose that was not present in the media used by Champomier-Verges

et al. (1996). MM9 enabled both satisfactory growth, as demonstrated by growth of F1801 at 25°C, while still ensuring conditions of iron-starvation, which can be seen by the strong increase in growth of F1801 in MM9 supplemented with 50 µM $FeCl_3$ (Fig 2A).

The sensitive CAS supernatant assay was used to detect the presence of siderophores in culture supernatants of F1801 grown at optimal growth temperature (25°C) in MM9. The CAS assay is based on the removal of iron from the chromogenic dye CAS by siderophores, whereby a colour change is observed from blue to orange (Schwyn and Neilands 1987). Figure 2B shows siderophores were clearly detected in cell-free supernatants of iron-starved cultures of F1801. Reaction times for the exchange of iron from CAS were within 1.5 h, a time-frame consistent with carboxylate-type siderophores (Schwyn and Neilands 1987). In contrast, when F1801 was grown in MM9 supplemented with 50 mM $FeCl_3$, siderophores were largely absent from culture supernatants (Fig 2B). Further, expression of the vibrioferrin genes was strongly down-regulated (between 12- (*pvsE*) and 120-fold (*pvsD*) reduction) relative to their expression in MM9 without iron-supplementation (Fig 2C), indicating repression of siderophore production under iron-rich conditions. These results are in agreement with other studies, which showed vibrioferrin production in *A. vinelandii*, *Xanthomonas* and *V. parahaemolyticus* increased under iron-limitation, while under iron-replete conditions vibrioferrin production ceased (Funahashi*, et al.* 2000, McRose*, et al.* 2017, Pandey and Sonti 2010, Pandey*, et al.* 2017). Thus, together with the presence of a putative Fur-box upstream of the vibrioferrin gene cluster, these results suggest Fur-mediated regulation of the *P. fragi* vibrioferrin genes.

As a key meat and milk spoilage bacterium, *P. fragi* F1801 was tested for siderophore production at refrigeration temperature by monitoring growth and the accumulation of siderophores in supernatants at 4°C over four days. Blue-coloured CAS solution has a maximum absorption at 630 nm. Orange-coloured CAS reaction mixtures, in which siderophores have removed iron from CAS, have essentially no absorbance at this wavelength and there is a largely linear dependence of A_{630}-values of CAS reaction mixtures versus concentration of the chelator (Schwyn and Neilands 1987). Figure 2D shows a steady decrease in A_{630} values of CAS reaction mixtures over the 4 days, indicating an accumulation of siderophores in culture supernatants of F1801. This accumulation correlated well with cell growth of the strain, demonstrating siderophore production of *P. fragi* at temperatures relevant to the storage of meat and milk.

To confirm a role for the vibrioferrin gene cluster in siderophore-mediated iron acquisition, a gene disruption mutant of the TonB-dependent outer membrane siderophore receptor (Δ*pvuA*) was generated, as well as a control strain with wild-type vibrioferrin genes and a disrupted lipase gene (Δ*lip*) for subsequent experimental comparisons. qRT-PCR analysis revealed that expression of genes downstream of *pvuA* in the Δ*pvuA* mutant was strongly reduced (between 7- (*pvsE*) and 128-fold (*pvsA*) reduction) relative to the Δ*lip* control strain (Fig 3A), indicating polar effects caused by integration of the suicide vector in the *pvuA* gene. As our aim was to confirm a role for this gene cluster in siderophore-mediated iron uptake, rather than to study the function of the vibrioferrin genes, which has been addressed in other studies (Fujita*, et al.* 2011, Funahashi*, et al.* 2002, Pandey and Sonti 2010, Pandey*, et al.* 2017, Tanabe*, et al.* 2003, Tanabe*, et al.* 2006), the Δ*pvuA* mutant was used for further investigations.

A strong reduction in siderophore levels was detected in culture supernatants of Δ*pvuA* compared to the Δ*lip* control strain (Fig 3B). Gene deletion of *pvuA*, which encodes an outer membrane vibrioferrin receptor, should result in an accumulation of siderophores in culture supernatants. Therefore the observed reduction was likely due to the polar effects on the downstream biosynthesis genes. Genetic variants were not found in genes or in non-coding regions associated with the vibrioferrin genes or other iron-related genes of the Δ*pvuA* mutant's genome (Table S2), demonstrating that phenotypes of the Δ*pvuA* mutant were solely due to the disruption of the target gene and associated polar effects.

A clear growth defect of the Δ*pvuA* mutant was not observed in MM9 when compared to the Δ*lip* control strain (Fig 4A). Therefore, to understand the role of the vibrioferrin siderophore under low iron conditions, growth of the Δ*pvuA* and Δ*lip* strains was tested under more severe iron-depleted conditions by adding 25 µM of the iron chelator 2,2'-bipyridyl (BP) to MM9. While growth of the Δ*lip* control strain was unaffected at 25 µM BP, addition of the ferrous iron chelator at these concentrations markedly impaired growth of the Δ*pvuA* mutant, demonstrating that the siderophore is involved in iron acquisition under low iron conditions.

To investigate whether the vibrioferrin siderophore could play a role in iron metabolism of *P. fragi* in foods such as meat and milk, where iron is sequestered by high-affinity iron-binding proteins, growth of Δ*pvuA* and Δ*lip* strains was compared in MM9, to which bovine apo-transferrin (apo-Tsf), as a model transferrin protein, was added. In all transferrin proteins, the carbonate (or bicarbonate) of the binding cleft is the synergistic anion, without which the protein loses its affinity for iron (Pakdaman and El Hage Chahine 1997). Thus, to ensure the specific binding of Fe^{3+} by apo-Tsf, the growth media was also supplemented with 20 mM bicarbonate (BC) (Chung

1984). BC at a concentration of 20 mM had no effect on the strains' growth when compared to their growth in MM9 without BC addition (Fig 4B). When the growth medium was supplemented with apo-Tsf at a concentration of 2.5 µM in the presence of 20 mM BC, growth, although slowed, was observed for the Δ*lip* control strain (Fig 4C). In contrast, growth of Δ*pvuA* was completely inhibited in the presence of apo-Tsf and BC, but could be rescued by supplementation of this media with 100 µM $FeCl_3$ (Fig 4D). These data suggest the vibrioferrin siderophore may be capable of removing ferric iron from transferrin proteins.

Remarkably, despite considerable divergence between the six vibrioferrin protein sequences shared by *A. vinelandii* and *V. parahaemolyticus*, the absence of an *mhpE* gene in *V. parahaemolyticus*, and the absence of the vibrioferrin-uptake genes *pvuA(1)-pvuE* in *A. vinelandii*, both bacteria were shown to produce identical vibrioferrin compounds (Baars*, et al.* 2016, Yamamoto*, et al.* 1994). Based on percent identities and the evolutionary relationship of the *P. fragi* vibrioferrin sequences with *A. vinelandii* and *V. parahaemolyticus* counterparts, it is likely that the *P. fragi* siderophore is an α-hydroxycarboxylate type siderophore, similar to or identical to vibrioferrin.

CONCLUSION

A vibrioferrin gene cluster was identified in 13 strains of the food spoilage bacterium *P. fragi* and siderophore production of *P. fragi* F1801 was observed. Based on the homology of the identified genes, *P. fragi* likely excretes an α-hydroxycarboxylate type siderophore, similar to or identical to vibrioferrin, which plays a role in iron-metabolism of this bacterium under low iron conditions. More experiments are required to determine whether the siderophore contributes to the successful growth

and colonisation of milk and meat by *P fragi*, however, these data suggest the vibrioferrin siderophore is capable of removing ferric iron from transferrin proteins.

FUNDING

This work was supported by the Australian Meat Processor Corporation (grant number 2013-5041) and the Commonwealth Scientific and Industrial Research Organisation (grant number OD-106390).

ACKNOWLEDGEMENT

We thank Steve Petrowski for providing plasmid pJP5603 and *Escherichia coli* strain S17-1 λpir.

***Conflicts of interest*:** None declared.

REFERENCES

Alexander DB, Zuberer DA. Use of chrome azurol S reagents to evaluate siderophore production by rhizosphere bacteria. Biol Fertility Soils 1991;**12**: 39-45.

Baars O, Zhang X, Morel FMM *et al.* The siderophore metabolome of *Azotobacter vinelandii*. Appl Environ Microbiol 2016;**82**: 27-39.

Blanvillain S, Meyer D, Boulanger A *et al.* Plant carbohydrate scavenging through TonB-dependent receptors: A feature shared by phytopathogenic and aquatic bacteria. PLoS ONE 2007;**2**: e224.

Blin K, Wolf T, Chevrette MG *et al.* antiSMASH 4.0-improvements in chemistry prediction and gene cluster boundary identification. Nucleic Acids Res 2017, DOI 10.1093/nar/gkx319.

Carpenter BM, Whitmire JM, Merrell DS. This is not your mother's repressor: The complex role of Fur in pathogenesis. Infect Immun 2009;**77**: 2590-601.

Casaburi A, Piombino P, Nychas G-J *et al.* Bacterial populations and the volatilome associated to meat spoilage. Food Microbiol 2015;**45, Part A**: 83-102.

Castresana J. Selection of conserved blocks from multiple alignments for their use in phylogenetic analysis. Mol Biol Evol 2000;**17**: 540-52.

Cezard C, Farvacques N, Sonnet P. Chemistry and biology of pyoverdines, *Pseudomonas* primary siderophores. Curr Med Chem 2015;**22**: 165-86.

Champomier-Vergès M-C, Stintzi A, Meyer J-M. Acquisition of iron by the non-siderophore-producing *Pseudomonas fragi*. Microbiology 1996;**142**: 1191-9.

Chung MC-M. Structure and function of transferrin. Biochemical Education 1984;**12**: 146-54.

Colombo C, Palumbo G, He J-Z *et al.* Review on iron availability in soil: Interaction of Fe minerals, plants, and microbes. J Soils Sed 2014;**14**: 538-48.

Cox CD, Adams P. Siderophore activity of pyoverdin for *Pseudomonas aeruginosa*. Infect Immun 1985;**48**: 130-8.

De Jonghe V, Coorevits A, Van Hoorde K *et al.* Influence of storage conditions on the growth of *Pseudomonas* species in refrigerated raw milk. Appl Environ Microbiol 2011;**77**: 460-70.

Faraldo-Gomez JD, Sansom MSP. Acquisition of siderophores in Gram-negative bacteria. Nat Rev Mol Cell Biol 2003;**4**: 105-16.

Farh ME-A, Kim Y-J, Sukweenadhi J *et al.* Aluminium resistant, plant growth promoting bacteria induce overexpression of Aluminium stress related genes in *Arabidopsis thaliana* and increase the ginseng tolerance against Aluminium stress. Microbiol Res 2017;**200**: 45-52.

Fujita MJ, Kimura N, Sakai A *et al.* Cloning and heterologous expression of the vibrioferrin biosynthetic gene cluster from a marine metagenomic library. Biosci, Biotechnol, Biochem 2011;**75**: 2283-7.

Funahashi T, Fujiwara C, Okada M *et al.* Characterization of *Vibrio parahaemolyticus* manganese-resistant mutants in reference to the function of the ferric uptake regulatory protein. Microbiol Immunol 2000;**44**: 963-70.

Funahashi T, Moriya K, Uemura S *et al.* Identification and characterization of *pvuA*, a gene encoding the ferric vibrioferrin receptor protein in *Vibrio parahaemolyticus*. J Bacteriol 2002;**184**: 936-46.

Garrity GM, Bell JA, Lilburn T. Pseudomonadales Orla-Jensen 1921, 270^{AL}. In: Brenner DJ, Krieg NR, Staley JT, Garrity GM, Boone DR, De Vos P, Goodfellow M, Rainey FA, Schleifer K-H (eds.) *Bergey's Manual® of Systematic Bacteriology: Volume Two The Proteobacteria Part B The Gammaproteobacteria*, DOI 10.1007/0-387-28022-7_9. Boston, MA: Springer US, 2005, 323-442.

Ilbert M, Bonnefoy V. Insight into the evolution of the iron oxidation pathways. Biochim Biophys Acta 2013;**1827**: 161-75.

Jones CM, Niederweis M. Role of porins in iron uptake by *Mycobacterium smegmatis*. J Bacteriol 2010;**192**: 6411-7.

Katoh K, Misawa K, Kuma K-i *et al.* MAFFT: a novel method for rapid multiple sequence alignment based on fast Fourier transform. Nucleic Acids Res 2002;**30**: 3059-66.

Kearse M, Moir R, Wilson A *et al.* Geneious Basic: an integrated and extendable desktop software platform for the organization and analysis of sequence data. Bioinformatics 2012;**28**: 1647-9.

McRose DL, Baars O, Morel FMM *et al.* Siderophore production in *Azotobacter vinelandii* in response to Fe-, Mo- and V-limitation. Environ Microbiol 2017;**19**: 3595-605.

Meyer JM, Abdallah MA. The fluorescent pigment of *Pseudomonas fluorescens*: Biosynthesis, purification and physicochemical properties. Microbiology 1978;**107**: 319-28.

Morariu VI, Srinivasan BV, Raykar V.C. *et al. Automatic online tuning for fast Gaussian summation*. Advances in Neural Information Processing Systems 21: Curran Associates, Inc., 2009.

Noinaj j, Guillier M, Travis J. Barnard *et al.* TonB-dependent transporters: Regulation, structure, and function. Annu Rev Microbiol 2010;**64**: 43-60.

Pakdaman R, El Hage Chahine J-M. Transferrin. Eur J Biochem 1997;**249**: 149-55.

Pandey A, Sonti RV. role of the FeoB protein and siderophore in promoting virulence of *Xanthomonas oryzae* pv. *oryzae* on rice. J Bacteriol 2010;**192**: 3187-203.

Pandey SS, Patnana PK, Rai R *et al.* Xanthoferrin, the alpha-hydroxycarboxylate-type siderophore of *Xanthomonas campestris* pv. *campestris*, is required for optimum virulence and growth inside cabbage. Mol Plant Pathol 2017;**18**: 949-62.

Penfold RJ, Pemberton JM. An improved suicide vector for construction of chromosomal insertion mutations in bacteria. Gene 1992;**118**: 145-6.

Rambaut A, Suchard MA, Xie D *et al.* Tracer v1.6. Available from http://treebioedacuk/software/tracer/ 2014.

Riedel T, Rohlfs M, Buchholz I *et al.* Complete sequence of the suicide vector pJP5603. Plasmid 2013;**69**: 104-7.

Ronquist F, Huelsenbeck JP. MrBayes 3: Bayesian phylogenetic inference under mixed models. Bioinformatics 2003;**19**: 1572-4.

Sambrook J, Russell DW. *Molecular cloning : A laboratory manual*. Cold Spring Harbor, N.Y: Cold Spring Harbor Laboratory, 2001.

Schwyn B, Neilands JB. Universal chemical assay for the detection and determination of siderophores. Anal Biochem 1987;**160**: 47-56.

Simon R, Priefer U, Puhler A. A broad host range mobilization system for in vivo genetic engineering: Transposon mutagenesis in gram negative bacteria. Nat Biotech 1983;**1**: 784-91.

Skaar EP. The battle for iron between bacterial pathogens and their vertebrate hosts. PLoS Path 2010;**6**: e1000949.

Stanborough T, Fegan N, Powell SM *et al.* Insight into the genome of *Brochothrix thermosphacta*, a problematic meat spoilage bacterium. Appl Environ Microbiol 2017;**83**: e02786-16.

Talavera G, Castresana J. Improvement of phylogenies after removing divergent and ambiguously aligned blocks from protein sequence alignments. Syst Biol 2007;**56**: 564-77.

Tanabe T, Funahashi T, Nakao H *et al.* Identification and characterization of genes required for biosynthesis and transport of the siderophore vibrioferrin in *Vibrio parahaemolyticus*. J Bacteriol 2003;**185**: 6938-49.

Tanabe T, Nakao H, Kuroda T *et al.* Involvement of the *Vibrio parahaemolyticus pvsC* gene in export of the siderophore vibrioferrin. Microbiol Immunol 2006;**50**: 871-6.

Trapet P, Avoscan L, Klinguer A *et al.* The *Pseudomonas fluorescens* siderophore pyoverdine weakens *Arabidopsis thaliana* defense in favour of growth in iron-deficient conditions. Plant Physiol 2016, DOI 10.1104/pp.15.01537.

Troxell B, Hassan HM. Transcriptional regulation by Ferric Uptake Regulator (Fur) in pathogenic bacteria. Front Cell Infect Microbiol 2013;**3**: 59.

Untergasser A, Cutcutache I, Koressaar T *et al.* Primer3--new capabilities and interfaces. Nucleic Acids Res 2012;**40**: e115.

Whelan S, Goldman N. A general empirical model of protein evolution derived from multiple protein families using a maximum-likelihood approach. Mol Biol Evol 2001;**18**: 691-9.

Windgassen M, Urban A, Jaeger K-E. Rapid gene inactivation in *Pseudomonas aeruginosa*. FEMS Microbiol Lett 2000;**193**: 201-5.

Yamamoto S, Okujo N, Yoshida T *et al.* Structure and iron transport activity of vibrioferrin, a new siderophore of *Vibrio parahaemolyticus*. J Biochem 1994;**115**: 868-74.

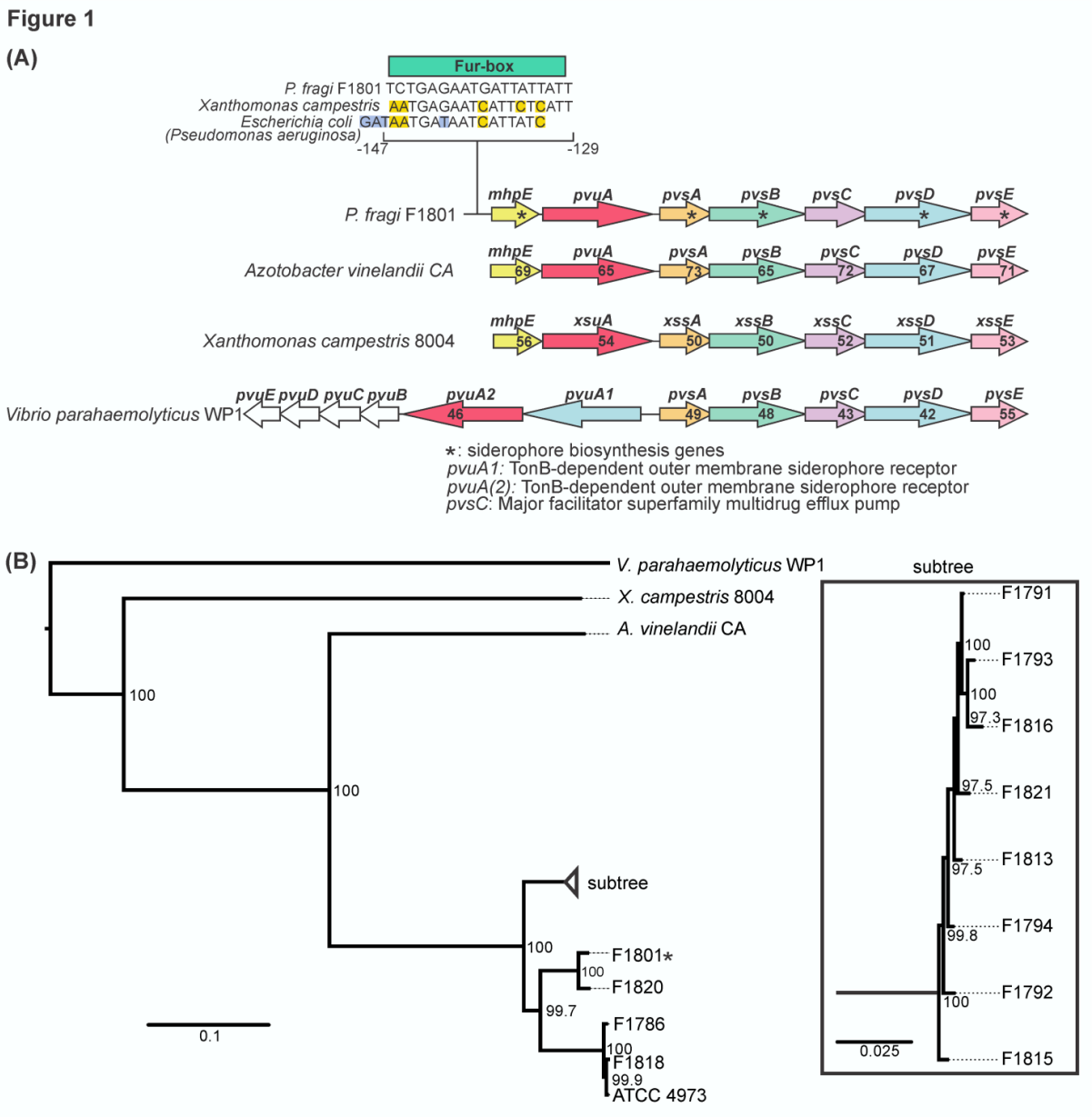

Figure 1. Vibrioferrin gene cluster identified in 13 *P. fragi*. (A) Schematic diagram of the vibrioferrin gene cluster identified in *P. fragi* and conserved synteny of these genes in known vibrioferrin producing bacteria *Azotobacter vinelandii*, *Xanthomonas campestris*, and *Vibrio parahaemolyticus*. Predicted biosynthesis genes are marked with an asterix in the *P. fragi* genes. Numbers shown in genes indicate percent sequence identity of proteins to respective homologs in *P. fragi* F1801, as determined by MAFFT protein alignment. The putative Fur-box identified upstream of the first gene in the *P. fragi* cluster is shown and consensus Fur-box

sequences of *X. campestris* and *Escherichia coli* (identical to the *Pseudomonas aeruginosa* consensus Fur-box) are included for comparison. **(B)** Mid-point rooted phylogram of the consensus BI tree of the PvuA and PvsA-PvsE sequences of the 13 *P. fragi*, *A. vinelandii*, *X. campestris* and *V. parahaemolyticus*. *P. fragi* F1801 that was used in subsequent experiments is marked with an asterix. The subtree shown in the box represents BI branching on a different scale to the tree. Posterior probability values are shown as percentages at the nodes and scale bars denote the number of substitutions per site.

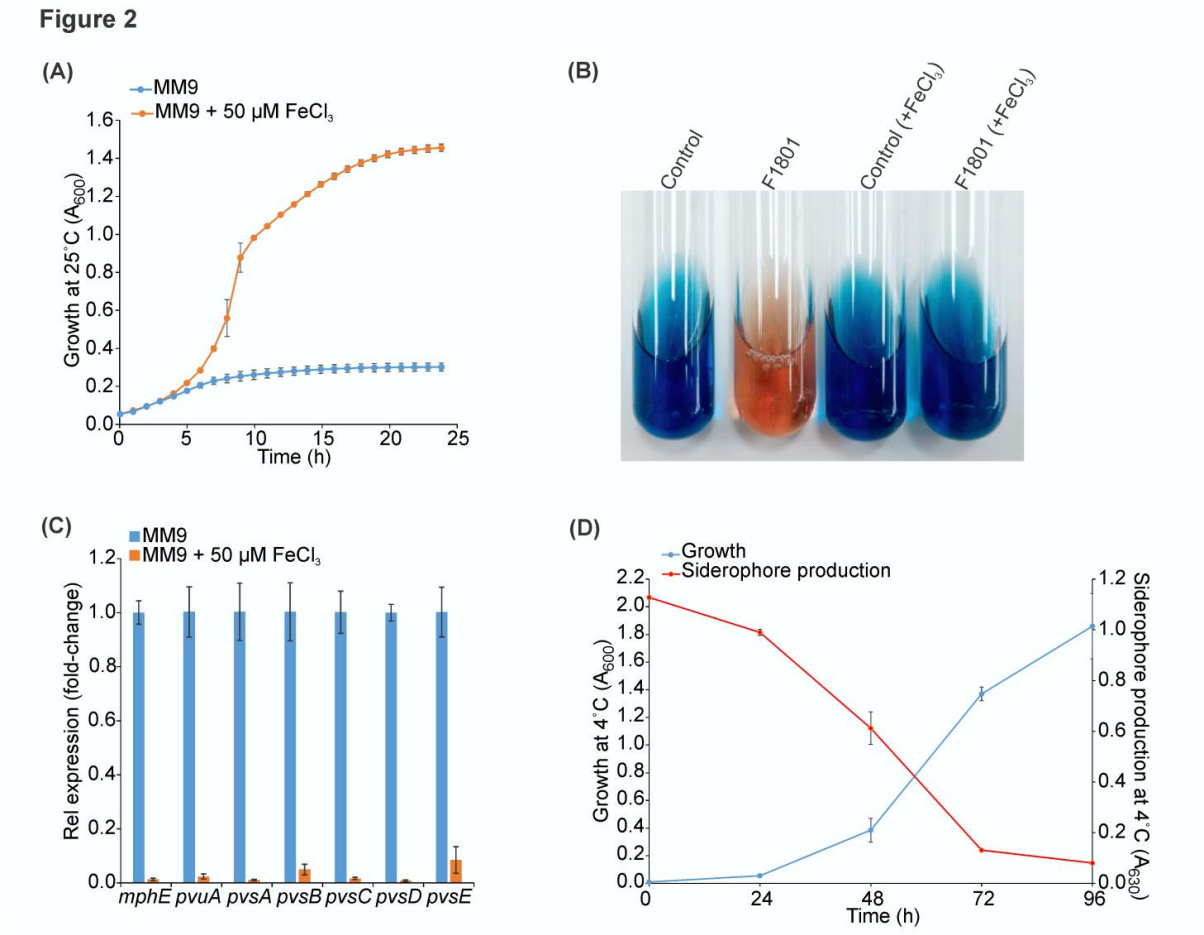

Figure 2. Siderophore production by *P. fragi* F1801 at 25°C and 4°C. (A) Growth of F1801 in MM9 or in MM9 that was supplemented with 50 µM $FeCl_3$. Optical density of the cultures was measured at 600 nm every hour in an EON microplate reader (BioTek). Data shown are the means and error bars the standard deviations

of three biological replicates. **(B)** CAS assay results of F1801. Shown from left to right is CAS solution that was added to; sterile MM9 (Control), filtered culture supernatant of F1801 grown in MM9 at 25°C (F1801), sterile MM9 supplemented with 50 µM $FeCl_3$ (Control (+$FeCl_3$)), and filtered culture supernatant of F1801 grown at 25°C in MM9 supplemented with 50 µM $FeCl_3$ (F1801 (+$FeCl_3$)). **(C)** Relative quantification by qRT-PCR of the vibrioferrin genes in F1801 under iron-replete conditions (MM9 supplemented with 50 µM $FeCl_3$) compared to conditions of iron-starvation (MM9). Data shown are the means and error bars the standard deviations of three biological replicates. **(D)** Growth of and siderophore production by F1801 in MM9 at 4°C. Optical density of the cultures and CAS assay absorbance measurements were carried out with a Novaspec Plus visible spectrophotometer (VWR). Data shown are the means and error bars the standard deviations of three biological replicates.

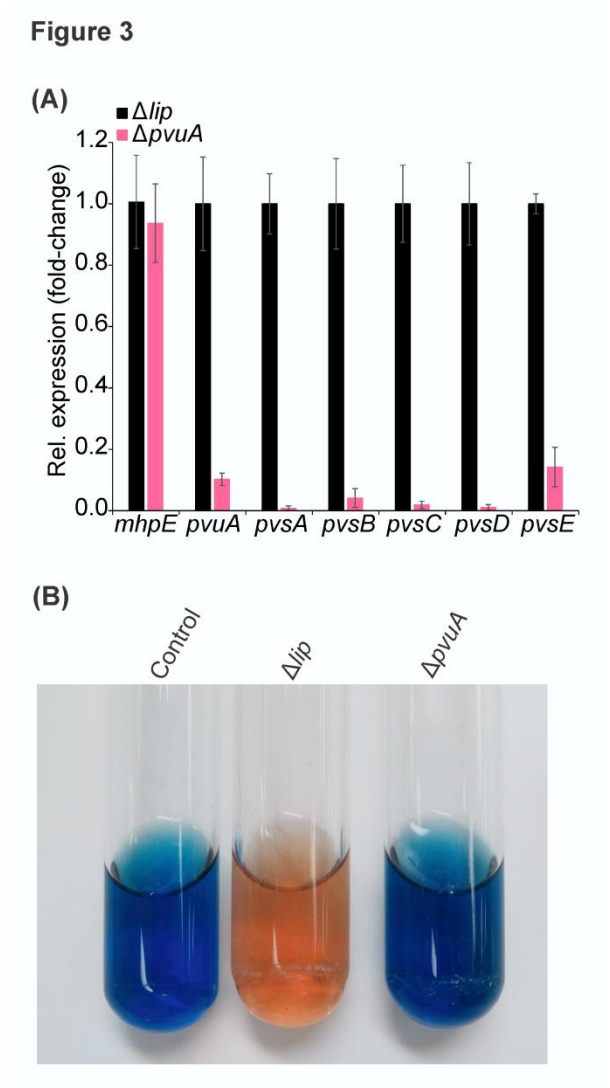

Figure 3. Δ*pvuA* shows impaired siderophore production. (A) Relative quantification by qRT-PCR of expression of the vibrioferrin genes in Δ*pvuA* compared with the Δ*lip* control strain. Data shown are the means and error bars the standard deviations of three biological replicates. **(B)** CAS assay results of the Δ*pvuA* mutant and Δ*lip* control strain. Shown from left to right is CAS solution that was added to; sterile MM9 (Control), filtered culture supernatant of Δ*lip* grown in MM9 at 25°C, and filtered culture supernatant of Δ*pvuA* grown in MM9 at 25°C.

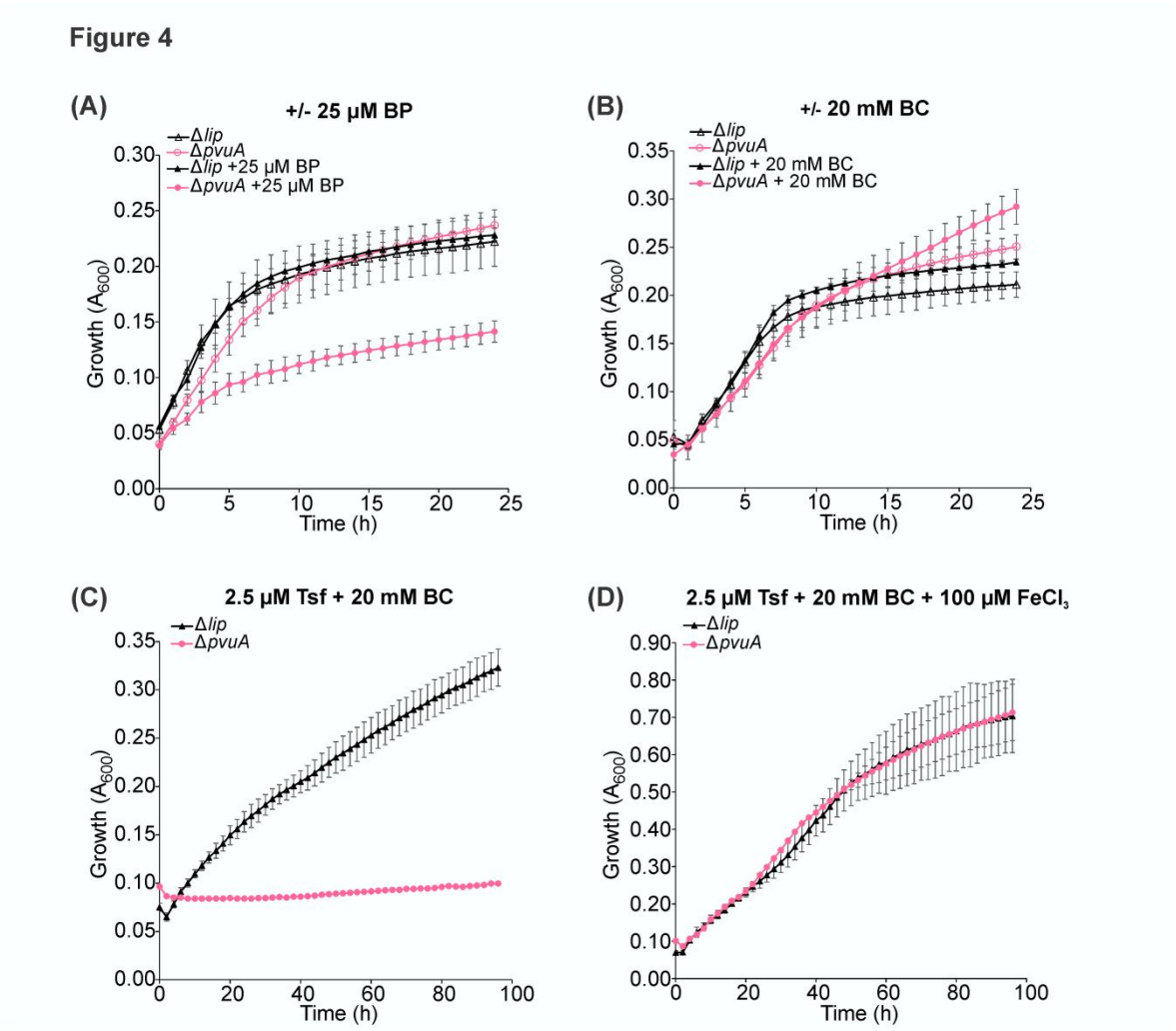

Figure 4. Vibrioferrin siderophore plays a role under iron-starvation and scavenges iron from transferrin. Growth of Δ*pvuA* and Δ*lip* control strain in MM9, and in MM9 supplemented with 25 µM 2,2'-bipyridyl (BP) **(A)**, in MM9, and in MM9 supplemented with 20 mM bicarbonate (BC) **(B)**, in MM9 supplemented with 2.5 µM bovine apo-transferrin (apo-Tsf) and 20 mM BC **(C)** and in MM9 supplemented with 2.5 µM apo-Tsf, 20 mM BC and 100 µM $FeCl_3$ **(D)**. Data shown for growth experiments in **(A)**, **(B)**, **(C)** and **(D)** are the means and error bars the standard deviations of three biological replicates. All experiments were repeated a minimum of three times with similar results observed.

Table 1. Strains, plasmids, and genome and gene sequences used in this study

Strains, plasmids, and genome and gene sequences	Relevant characteristics	Locus tags of vibrioferrin genes	Accession numbers[a]
***Pseudomonas fragi* genome sequences**			
F1786[b]		CJU73_02415 - CJU73_02445	GCA_002269585.1
F1791[b]		CJU79_02430 - CJU79_02400	GCA_002269515.1
F1792[b]		CJU72_13900 - CJU72_13930	GCA_002269595.1
F1793[b]		CJU75_07595 - CJU75_07565	GCA_002269565.1
F1794[b]		CJU80_05030 - CJU80_05000	GCA_002269445.1
F1813[b]		CJU77_09910 - CJU77_09940	GCA_002269465.1
F1815[b]		CJU76_02305 - CJU76_02275	GCA_002269545.1
F1816[b]		CJU74_06845 - CJU76_06815	GCA_002269485.1
F1818[b]		CJU78_20565 - CJU78_20595	GCA_002269625.1
F1820[b]		CJF43_16240 - CJF43_16270	GCA_002269055.1
F1821[b]		CJF37_06830 - CJF37_06800	GCA_002269155.1
ATCC 4973[b]		SAMN05216594_0902 - SAMN05216594_0896	GCA_900105835.1
F1801[b]		CJU81_14170 - CJU81_14200	GCA_002269505.1
***Pseudomonas fragi* strains**			
F1801[c]	Wild-type		SRX3235903
F1801Δ*lip*[c]	Disruption of CJU81_12870[b] at 167th amino acid encoding codon, Km^{r}		SRX3235904
F1801Δ*pvuA*[c]	Disruption of CJU81_14195[b] at 419th amino acid encoding codon, Km^{r}		SRX3235905

***Escherichia coli* strains**			
Escherichia coli S17-1 *λpir*	*thi*, *pro*, *hsd* (r^- m^+) *recA*::RP4-2-Tc^r::Mu Km^r::Tn7 Tp^r Sm^r *λpir*		
Genome/gene sequences of other bacteria			
Azotobacter vinelandii CA			GCA_000380335.1
Xanthomonas campestris 8004			GCA_000012105.1
Vibrio parahaemolyticus WP1			AB048250.2 and AB082123.1
Plasmids			
pJP5603	*Suicide plasmid, Km^r*		
pJP5603_lip323-783	pJP5603::disruption construct for gene CJU81_12870[c], Km^r		
pJP5603_pvuA886-1523	pJP5603::disruption construct for gene CJU81_14195[c], Km^r		

[a] Relevant GenBank and Sequence Read Archive accession numbers provided.

[b] Previously sequenced *P. fragi* genomes that were examined for the presence of siderophore biosynthetic gene clusters.

[c] Genomes sequenced in this study.

[d] Locus tags of respective coding sequences.